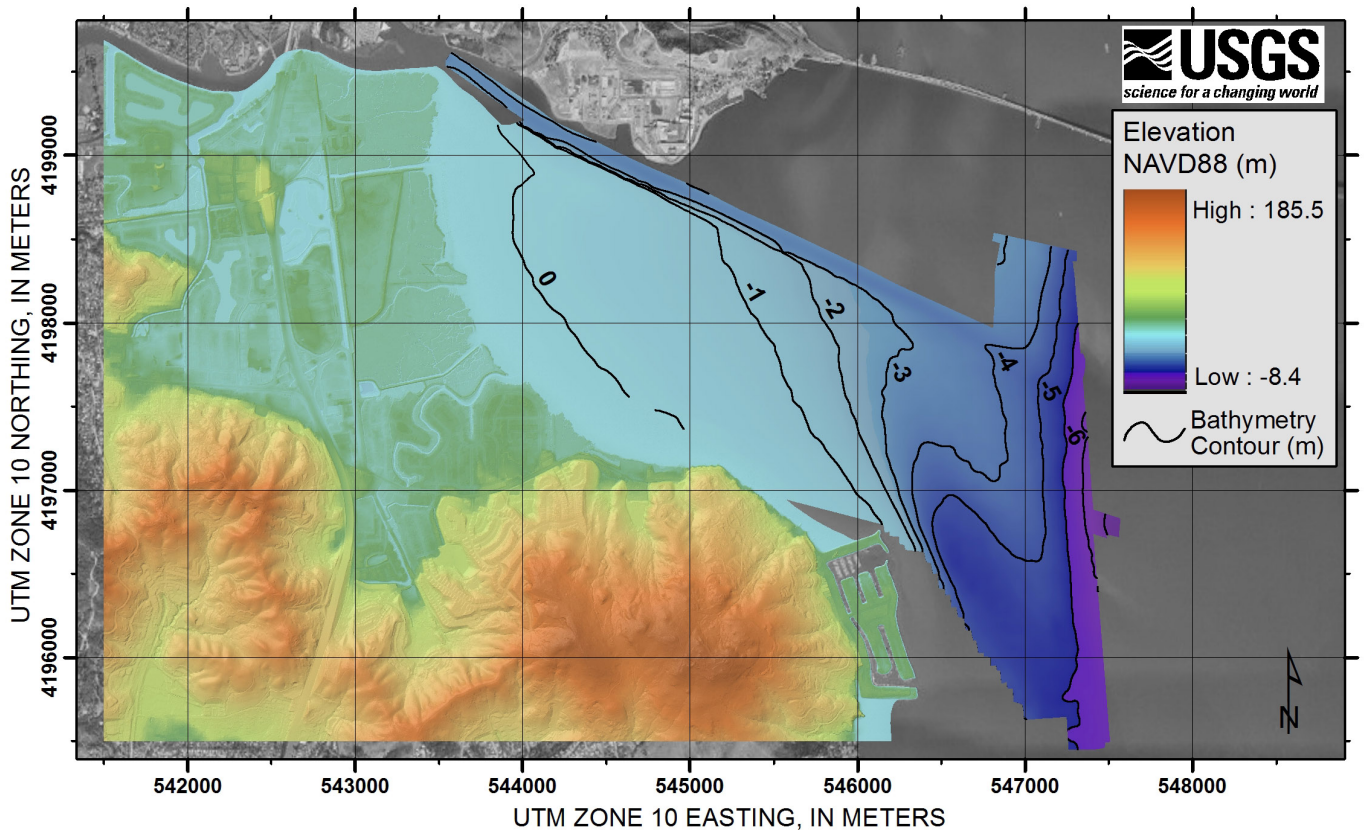




2010 Bathymetric Survey and Digital Elevation Model of Corte Madera Bay, California

By Amy C. Foxgrover, David P. Finlayson, Bruce E. Jaffe, John Y. Takekawa, Karen M. Thorne, and Kyle A. Spragens



Open-File Report 2011-1217

U.S. Department of the Interior
U.S. Geological Survey

U.S. Department of the Interior
KEN SALAZAR, Secretary

U.S. Geological Survey
Marcia K. McNutt, Director

U.S. Geological Survey, Reston, Virginia: 2011

For product and ordering information:
World Wide Web: <http://www.usgs.gov/pubprod>
Telephone: 1-888-ASK-USGS

For more information on the USGS—the Federal source for science about the Earth,
its natural and living resources, natural hazards, and the environment:
World Wide Web: <http://www.usgs.gov>
Telephone: 1-888-ASK-USGS

Suggested citation:
Foxgrover, A.C., Finlayson, D.P., Jaffe, B.E., Takekawa, J.Y., Thorne, K.M., and Spragens, K.A., 2011, 2010
bathymetric survey and digital elevation model of Corte Madera Bay, California: U.S. Geological Survey Open-File
Report 2011-1217, 20 p., available at <http://pubs.usgs.gov/of/2011/1217/>.

Any use of trade, product, or firm names is for descriptive purposes only and does not imply
endorsement by the U.S. Government.

Although this report is in the public domain, permission must be secured from the individual
copyright owners to reproduce any copyrighted material contained within this report.

Cover: Seamless bathymetric/topographic DEM of Corte Madera, California; from figure 12

Contents

Abstract.....	1
Introduction.....	1
Data Collection.....	1
Geodetic Control.....	4
Sound Velocity Measurements.....	4
Processing Procedures.....	5
Real-time Sonar Sounding Processing.....	6
Swath Cleaning and Filtering.....	6
Water-Column Artifacts in S-3-10-SF.....	6
Horizontal and Vertical Datum Conversions.....	9
Estimates of Bathymetric Uncertainty.....	10
Digital Elevation Model Production.....	13
Bathymetric Grids.....	13
Lidar Data.....	14
Bathymetric / Topographic DEM.....	14
Evaluation of Lidar Bare Earth Elevations in Marsh Vegetation.....	16
Data Tables.....	18
A Note on Coordinate Systems and Datums.....	18
Bathymetry.....	18
Bathymetric / Topographic DEM.....	18
Acknowledgments.....	19
References Cited.....	19
Appendix.....	20

Figures

1. Map of study area, Corte Madera Bay, California.....	2
2. U.S. Geological Survey, Coastal and Marine Geology Research Vessel <i>Parke Snavely</i>	2
3. Fore and aft views of the SWAT Hplus sonar pole mount on the R/V <i>Snavely</i>	3
4. Processing workflow diagram for converting soundings to a digital elevation model (DEM).....	5
5. Sample cross-sectional views of sounding swaths within CARIS demonstrating typical sounding distributions upon a flat surface and curvatures resulting from refraction artifacts.....	7
6. 1-m resolution bathymetry grid generated by merging surveys S-3-10-SF and S-9-10-SF.....	8
7. 1-m resolution bathymetry grid with interpolation performed to fill the gaps between tracklines.....	9
8. Histogram of sounding elevation standard deviations within each 1 by 1 m cell.....	11
9. Plan-view map of bathymetric soundings standard deviation within each 1 by 1 m cell.....	11
10. Uncertainty in sounding elevation compared to IHO standards as a function of water depth.....	13
11. Difference between tidal flat elevations calculated from aerial lidar versus bathymetry.....	15
12. Seamless bathymetric/ topographic DEM of Corte Madera.....	16
13. Comparison between RTK GPS ground-truth measurements and bare earth lidar elevations.....	17

Tables

1. SWATHplus-M Sonar Specifications (SEALtd., 2004).....	4
2. National Geodetic Survey OPUS solutions for Corte Madera GPS base station CM01.....	4
3. Parameters adopted for transformation between WGS84 (G1150) and NAD83 (CORS96).....	10
4. Minimum IHO survey order requirements.....	12
5. Difference statistics between RTK measurements and bare earth lidar elevations in the marsh.....	17
6. Bathymetric data files provided.....	18
7. Bathymetric/topographic DEM files provided.....	19

Conversion Factors

Multiply	By	To obtain
Length		
inch (in.)	2.54	centimeter (cm)
inch (in.)	25.4	millimeter (mm)
foot (ft)	0.3048	meter (m)
mile (mi)	1.609	kilometer (km)
mile, nautical (nmi)	1.852	kilometer (km)
yard (yd)	0.9144	meter (m)
Area		
acre	4,047	square meter (m ²)
acre	0.4047	hectare (ha)
acre	0.4047	square hectometer (hm ²)
acre	0.004047	square kilometer (km ²)
square foot (ft ²)	929.0	square centimeter (cm ²)
square foot (ft ²)	0.09290	square meter (m ²)
square inch (in ²)	6.452	square centimeter (cm ²)
section (640 acres or 1 square mile)	259.0	square hectometer (hm ²)
square mile (mi ²)	259.0	hectare (ha)
square mile (mi ²)	2.590	square kilometer (km ²)

2010 Bathymetric Survey and Digital Elevation Model of Corte Madera Bay, California

By Amy C. Foxgrover¹, David P. Finlayson¹, Bruce E. Jaffe¹, John Y. Takekawa², Karen M. Thorne², and Kyle A. Spragens²

¹USGS Pacific Science Center, Santa Cruz, Calif.

²USGS Western Ecological Research Center, Vallejo, Calif.

Abstract

A high-resolution bathymetric survey of Corte Madera Bay, California, was collected in early 2010 in support of a collaborative research project initiated by the San Francisco Bay Conservation and Development Commission and funded by the U.S. Environmental Protection Agency. The primary objective of the Innovative Wetland Adaptation in the Lower Corte Madera Creek Watershed Project is to develop shoreline adaptation strategies to future sea-level rise based upon sound science. Fundamental to this research was the development of an up-to-date, high-resolution digital elevation model (DEM) extending from the subtidal environment through the surrounding intertidal marsh. We provide bathymetric data collected by the U.S. Geological Survey and have merged the bathymetry with a 1-m resolution aerial lidar data set that was collected by the National Oceanic and Atmospheric Administration during the same time period to create a seamless, high-resolution DEM of Corte Madera Bay and the surrounding topography. The bathymetric and DEM surfaces are provided at both 1 m and 10 m resolutions formatted as both X, Y, Z text files and ESRI Arc ASCII files, which are accompanied by Federal Geographic Data Committee compliant metadata.

Introduction

Data Collection

Corte Madera Bay is located in the northwestern portion of Central San Francisco Bay, California, just south of the Richmond-San Rafael Bridge (fig. 1). Two separate bathymetric surveys of Corte Madera Bay were completed: the first (USGS Field Activity ID: [S-3-10-SF](#)) from January 26-29, 2010 and the second (USGS Field Activity ID: [S-9-10-SF](#)) on March 29-30, 2010. The combined bathymetric surveys consist of 215 survey lines covering an area of approximately 6.5 km² extending north to the dredged ferry channel leading to Corte Madera Creek and to the south, just beyond Paradise Cay Yacht Harbor. Both surveys were done aboard the research vessel R/V *Parke Snavely*, a state-of-the-art research vessel outfitted with a pole-mounted 234.5 kHz SEA (Systems Engineering & Assessment Ltd.) SWATHplus-M phase-differencing sidescan sonar (figs. 2 and 3). Real-time kinematic (RTK) GPS position data were passed through a CodaOctopus F180 inertial measurement unit (IMU) to the sonar hardware and data collection software. Sonar heads, GPS antennae, and the IMU were surveyed in place to a common reference frame with a Geodimeter 640 Total Station. The R/V *Snavely* was outfitted with three networked workstations and a navigation computer for use by the captain and survey crew for data collection and initial processing. See table 1 for the sonar system specifications.

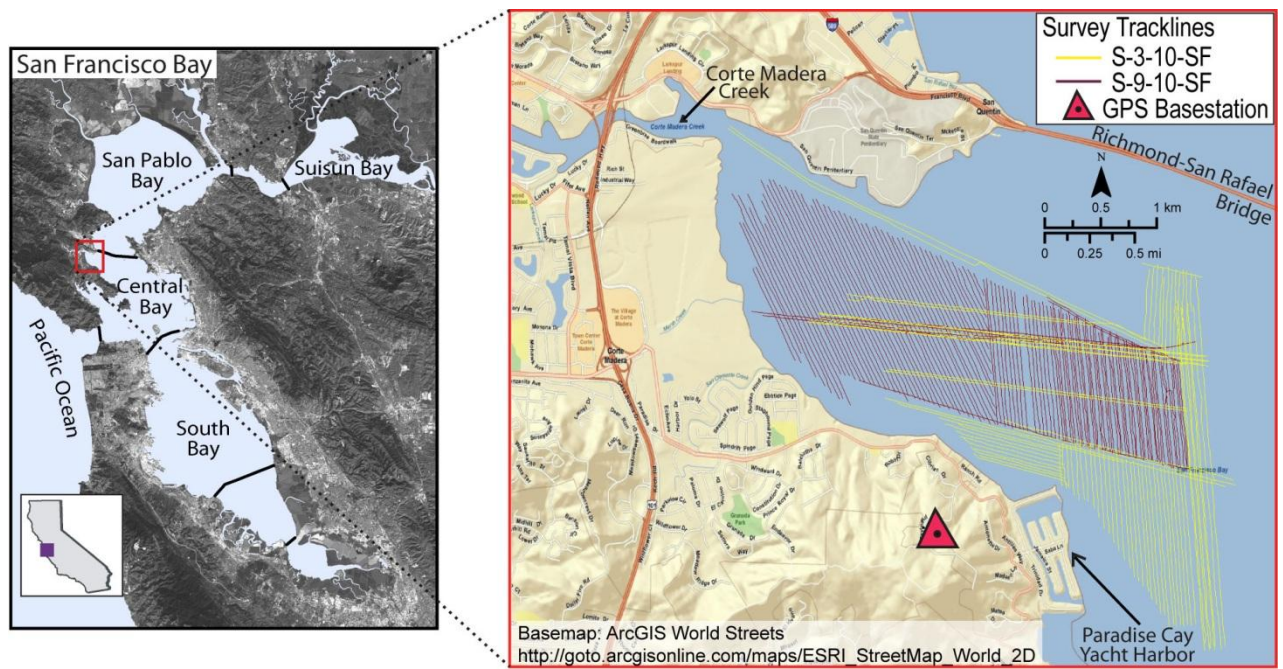


Figure 1. Location map of study area, Corte Madera Bay, California, with bathymetric survey tracklines colored by cruise ID.



Figure 2. U.S. Geological Survey, Coastal and Marine Geology Research Vessel *Parke Snavely*. Photo courtesy of Thomas E. Reiss.



Figure 3. Fore and aft views of the SWATHplus sonar pole mount on the RV *Snavelly*.

Table 1. SWATHplus-M Sonar Specifications (SEA Ltd., 2004).

Sonar frequency	234.5 kHz
Maximum water depth	120 m
Maximum swath width	300 m (typically 7 to 12 times water depth)
Resolution across track (best case)	5 cm
Transmit pulse length	34 ms to 500 ms
Ping repetition rate	
150 m swath width	10 pings per second
300 m swath width	5 pings per second
Vertical accuracy (range dependent)	
57 m	0.1 m
114 m	0.2 m
171 m	0.3 m

Geodetic Control

Geodetic control for the survey was established using a shore-based GPS base station broadcasting RTK corrections to the survey vessel by UHF radio link. The GPS base station (CM01) was established in the nearby hills along Taylor Drive (see figure 1). The average National Geodetic Survey (NGS) Online Positioning User Server (OPUS) solutions for CM01 are provided in table 2.

Table 2. National Geodetic Survey OPUS solutions for Corte Madera GPS base station CM01.

Reference frame	WGS84 (G1150) (same as ITRF00)	NAD83, UTM zone 10
Epoch	2010.1532	2002.0000
Latitude / Northing	N 37° 54' 51.37819"	4196426.825 m
Longitude / Easting	W 122° 29' 13.21786"	545093.607 m
Ellipsoid height	88.780 m	89.310 m
Orthometric height	N/A	121.651 m (based on GEOID09)

The R/V Snively was equipped with a CodaOctopus F180 attitude and positioning system for the duration of the survey. The F180 is running F190 firmware and receives RTK corrections directly. The RTK GPS data (2 cm error ellipse) are combined with the inertial motion measurements directly within the F190 hardware so that high-precision position and attitude corrections are fed in real time to the sonar acquisition equipment. The WGS84 (G1150)/ITRF 2000 reference frame was used for both horizontal and vertical positioning. In post-processing, the data was converted to orthometric heights NAD83 (CORS96)/NAVD88 (see processing procedures section below). All data is projected in UTM coordinate space in meters, zone 10 north.

Sound Velocity Measurements

Sound-velocity measurements were collected continuously with an Applied Micro Systems Micro SV (accurate to ± 0.03 m/s) deployed on the transducer frame for real-time sound-velocity

adjustments at the transducer/water interface. Additionally, sound-velocity profile measurements of the water column were collected at the beginning and ending of each survey day and when there were large changes in water depth (that is, when transitioning from collecting data in the channels to the tidal flats or vice versa). Sound-velocity profile measurements were collected using an Applied Micro Systems SvPlus 3472, which provides time-of-flight sound-velocity measurements using invar rods with a sound-velocity accuracy of ± 0.06 m/s. Pressure was measured by a semiconductor bridge strain gauge to an accuracy to 0.15 percent (full scale), and temperature measured by thermistor to an accuracy of 0.05 C (Applied Microsystems Ltd., 2005).

Processing Procedures

The general processing work-flow procedures for converting raw bathymetric soundings to a DEM are shown in figure 4. Critical aspects of the processing procedure are discussed in more detail below.

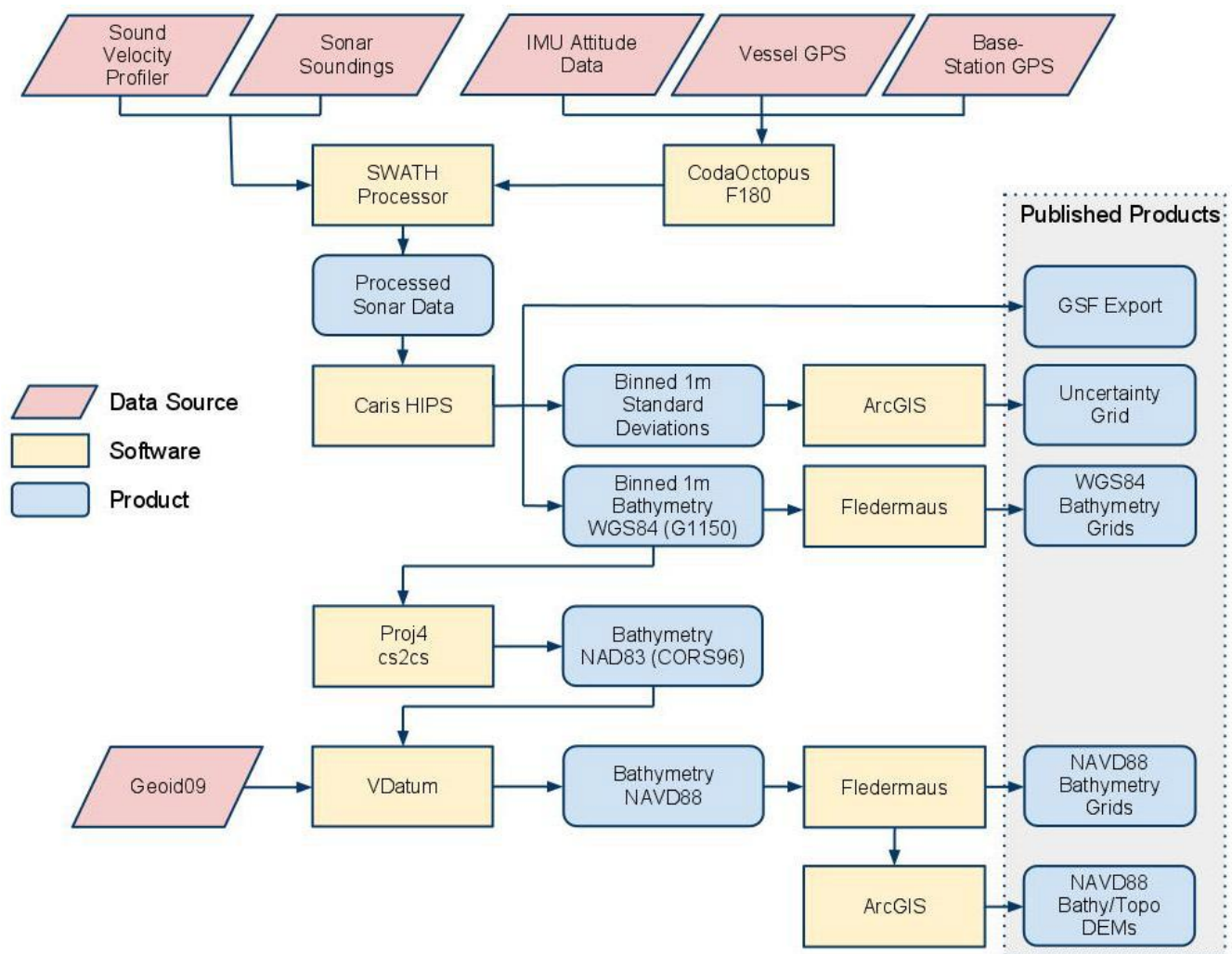


Figure 4. Processing workflow diagram for converting soundings to a digital elevation model (DEM).

Real-time Sonar Sounding Processing

GPS data and measurements of vessel motion are combined in the F180 hardware to produce a high-precision vessel attitude packet. This packet is transmitted to the Swath Processor acquisition software in real-time and combined with instantaneous sound-velocity measurements at the transducer head before each ping. Up to 20 pings per second are transmitted with each ping consisting of 2,048 samples per side (port and starboard). The returned samples are projected to the seafloor using a ray-tracing algorithm working with the previously measured sound-velocity profiles in SEA Swath Processor (version 3.05.18.04). A series of statistical filters are applied to the raw samples that isolate the seafloor returns from other uninteresting targets in the water column. Finally, the processed data is stored line-by-line in both raw (.sxr) and processed (.sxp) trackline files. For these surveys, processed files were filtered across-track with a mean filter at 0.2 m resolution.

Swath Cleaning and Filtering

The processed .sxp files were imported to CARIS HIPS and SIPS (version 7.0.1.0 Service Pack 1) for additional cleaning and filtering. Swath filters were applied to clean the data based upon characteristics such as depth, across-track angle, and across-track distance. A CARIS Swath Angle BASE (Bathymetric with Associated Statistical Error) surface was created at 1 m resolution, and the subset editor was used to manually eliminate remaining outliers or artifacts. The average depth within each 1 by 1 m cell was exported as an ASCII text file along with calculations of the bin standard deviation (of all soundings within the 1 m by 1 m cell spacing) and the sounding density.

Water-Column Artifacts in S-3-10-SF

It became apparent during the January bathymetric cruise (S-3-10-SF) that the sound ray-tracing algorithm used by the SWATHplus software was calculating some sounding ranges and/or angles improperly. This situation usually is the result of a bad sound-velocity model for the water column and results in (sound) refraction artifacts which manifest themselves as curvatures (either upwards or downwards) in the across-profile depth solutions. Curvature becomes more pronounced with increased distance from nadir. The usual remedy to this problem is to re-measure the sound-velocity profile and to recalculate the ray-tracing model; however, despite the collection of numerous sound-velocity profiles, we were not able to eliminate the refraction errors. We suspect that a strong storm system that moved through the region the week prior to the survey affected the water-column properties of the bay in a complex way. Properties such as salinity, temperature, and sediment concentration, which all affect sound velocity, could have been influenced by increased freshwater input to the bay through surface runoff, accidental sewage overflow, or through ground-water efflux. The sound-velocity profile measurements taken aboard the vessel were insufficient to characterize the spatial variability of sound velocity throughout the study area, which in turn compromised the ability of the sonar to properly ray-trace the soundings to the seafloor. Fortunately, refraction artifacts are a function of slant-range and angle of incidence, so that soundings directly beneath the vessel are less affected than the off-nadir soundings.

At the time of collection, six sidescan surveys had been completed in similar settings within San Francisco Bay using the identical system configuration, and this was the first time that refraction artifacts were a problem. Furthermore, the identical setup was used for the second cruise just two months later, and the refraction artifacts did not appear, which leads us to believe that the artifacts were a function of water-column properties at the time of the survey. As a result, during the post-processing of S-3-10-SF within CARIS, the bathymetric swath was trimmed to retain only those soundings within

close proximity to nadir so as to minimize any refraction artifacts (fig. 5). The accuracy of the retained soundings from S-3-10-SF was verified by differencing the north/south oriented tracklines from the intersecting east/west oriented tracklines collecting during S-9-10-SF. The intersecting tracklines had a mean offset of 5 cm (SD=6) and a maximum difference of up to 61 cm. These differences fall within the accuracy of the system (discussed further in the section “estimates of bathymetric uncertainty”) and within the anticipated scale of geomorphic change that could occur within the two months between surveys. Owing to the aggressive trimming of data to eliminate refraction artifacts, there is not 100 percent overlap with adjacent tracklines for S-3-10-SF, resulting in narrow data gaps (~15 m wide) between some survey lines when the data is exported at 1 m cell size (fig. 6). Fortunately, the majority of tracklines displaying the refraction artifact were within the intertidal flats, and although the across-swath trimming of data left gaps between adjacent tracklines, the gently sloping terrain is highly conducive to interpolating across these gaps (fig. 7).

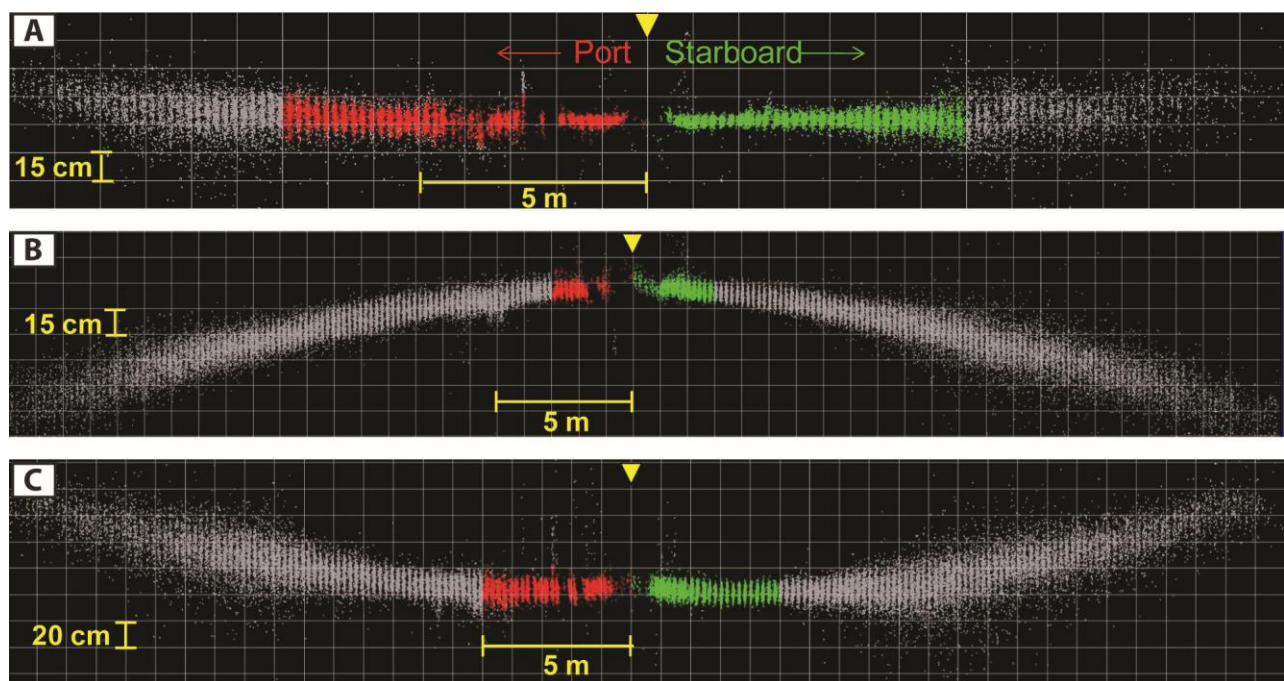


Figure 5. A cross-sectional view looking along-swath at soundings edited by individual trackline in CARIS. The yellow triangle represents the location of the transducer with soundings on the left (port side) and right (starboard) side of the boat. Gray dots represent all of the potential solutions for depth soundings, and the colored dots (red for port and green for starboard) represent soundings retained after filtering and manually cleaning the data in CARIS. *A*, A typical shallow-water profile collected in the intertidal flats, with scatter increasing uniformly with distance from nadir. *B*, A sample taken from S-3-10-SF where refraction artifacts result in an underestimate of surface elevation increasing with distance from nadir. *C*, A sample taken from S-3-10-SF where refraction artifacts result in an overestimate of surface elevation increasing with distance from nadir.

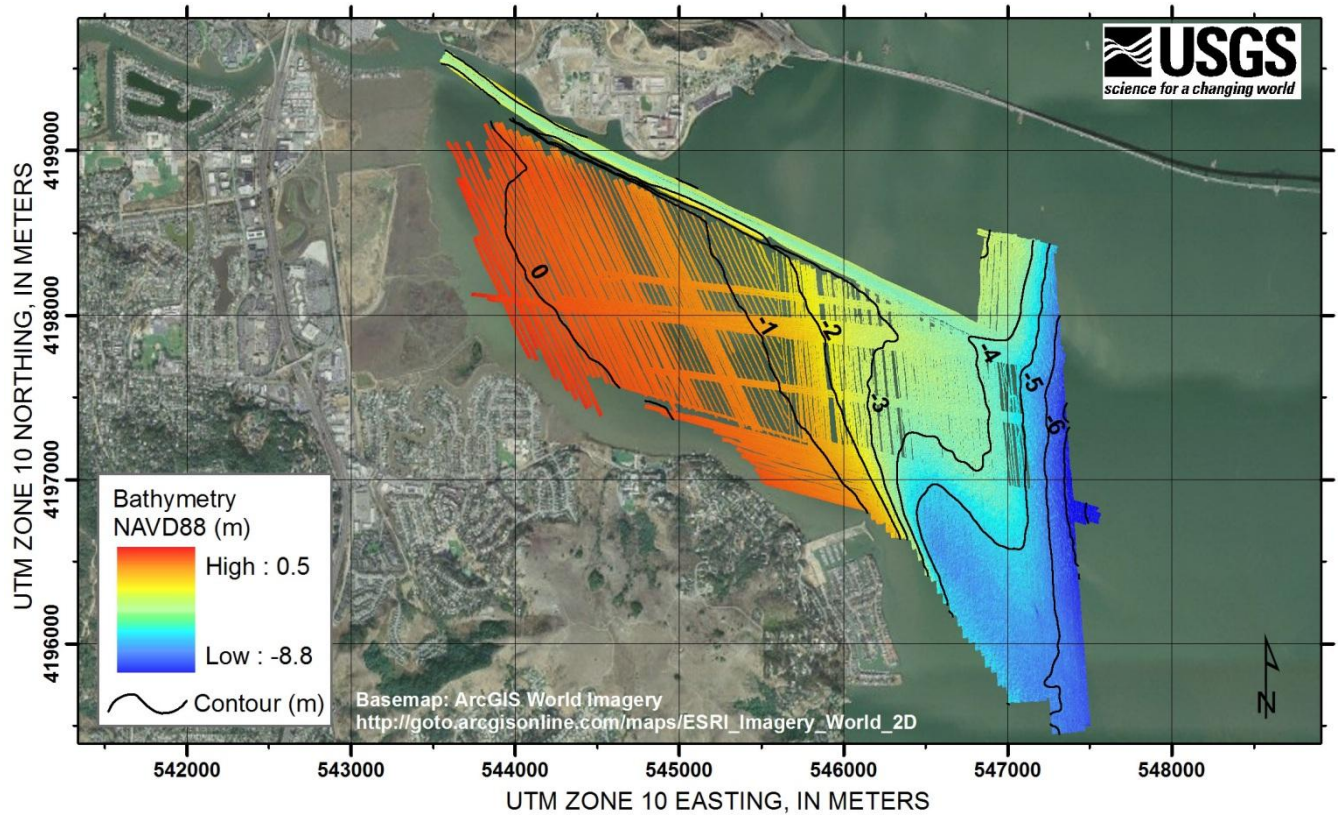


Figure 6. 1-m resolution bathymetry grid generated by merging surveys S-3-10-SF and S-9-10-SF, Corte Madera Bay, California. Narrow gaps between tracklines exist as a result of trimming across-swath widths to eliminate refraction artifacts.

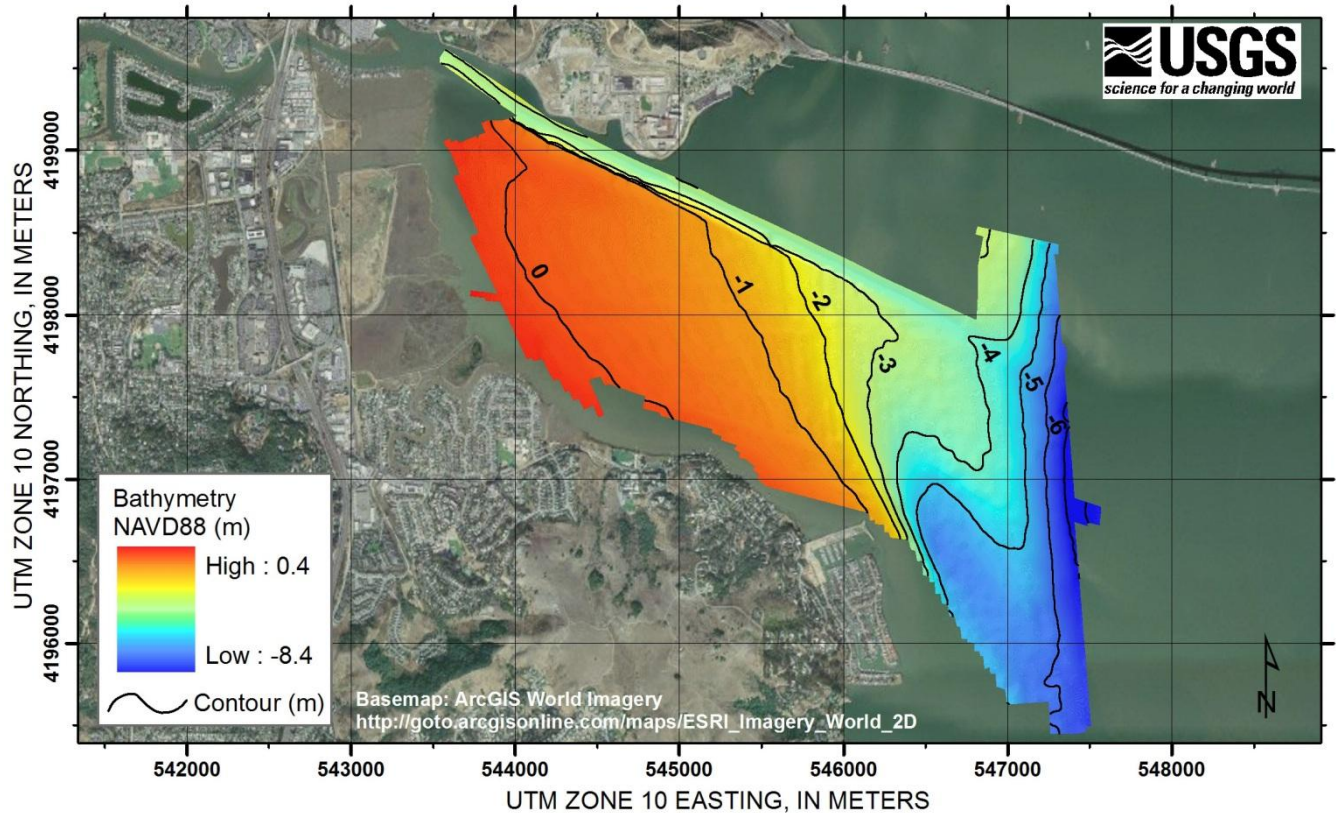


Figure 7. 1-m resolution bathymetry grid generated using a weighted moving average gridding algorithm, with a search diameter of 100 m, to interpolate across gaps between tracklines, Corte Madera Bay, California.

Horizontal and Vertical Datum Conversions

To convert the data from the WGS84 (G1150) ellipsoid to NAD83 (CORS96), the 1-m grid resolution data was exported from CARIS to an X, Y, Z point file. Next, a 14-point Helmert transformation was applied with time-dependent transformation parameters figured for January 23, 2010, according to methods outlined in Soler and Snay (2004). Table 3 shows the specific parameters in the format required by the cs2cs program found in the Proj4 library used to transform the points. The NAD83 (CORS96) ellipsoid elevations were then converted to orthometric heights based on NAVD88 and the National Geodetic Survey (NGS) Geoid09 Model (National Geodetic Survey, 2009) in VDatum v 2.3.0 (<http://vdatum.noaa.gov/>).

Table 3. Parameters adopted for transformation between WGS84 (G1150) and NAD83 (CORS96).

Parameter	Definition	Units	Value at $t_0=1997.0$	Value at $t_f=2010.0630$
T_x	x-shift	meters	0.9956	1.0047
T_y	y-shift	meters	-1.9013	-1.9104
T_z	z-shift	meters	-0.5215	-0.5150
ω_x	x-rotation ¹	arc seconds	0.025915	-0.026790
ω_y	y-rotation ¹	arc seconds	0.009426	.000461
ω_z	z-rotation ¹	arc seconds	0.011599	-0.010933
S	scale	parts-per-million	0.00062	-0.00173

¹Note that the Proj4 program cs2cs reverses the sign of the rotation parameters from the Soler and Snay (2004) algorithm.

Estimates of Bathymetric Uncertainty

For relatively flat portions of the seafloor, the standard deviation of sounding elevations within a small area is a good measure of the precision of the sonar instrumentation; this is not true in areas where the seafloor is naturally variable or steep. In these areas, the standard deviation reflects the combination of natural variation of the surface, and sonar measurement uncertainty. After post-processing the data in CARIS to remove obvious outliers, the standard deviation of the soundings within each 1 by 1 m cell (containing more than 400 soundings on average) was calculated. The mean of the standard deviation for all of the cells in the survey is 0.06 m, and 98 percent of the cells have a standard deviation less than 0.15 m (fig. 8). These absolute numbers are a good indication of the distribution of uncertainty in bathymetric soundings, however, measurement errors naturally increase with range from the system (that is, with increasing depth). A plan-view map of spatial variability in standard deviations throughout the study area is shown in figure 9. Although slightly higher standard deviations exist in the tidal flats along the west/easterly oriented tracklines, this can likely be attributed to actual changes in bed elevation during the two month timespan between surveying the overlapping tracklines. The overall spatial pattern of standard deviation reveals low standard deviation in the low-relief intertidal flats and increases with increasing depth and slope of the bay floor. This highlights the need for a measure of survey reliability that accounts for water depth as a factor. The International Hydrographic Organization (IHO) standards described next provide such a metric.

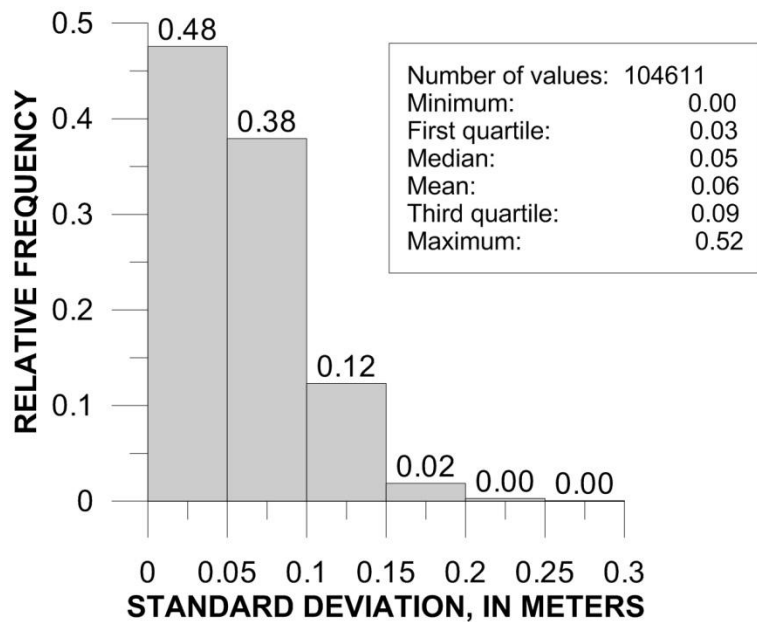


Figure 8. Histogram of sounding elevation standard deviations within each 1 by 1 m cell.

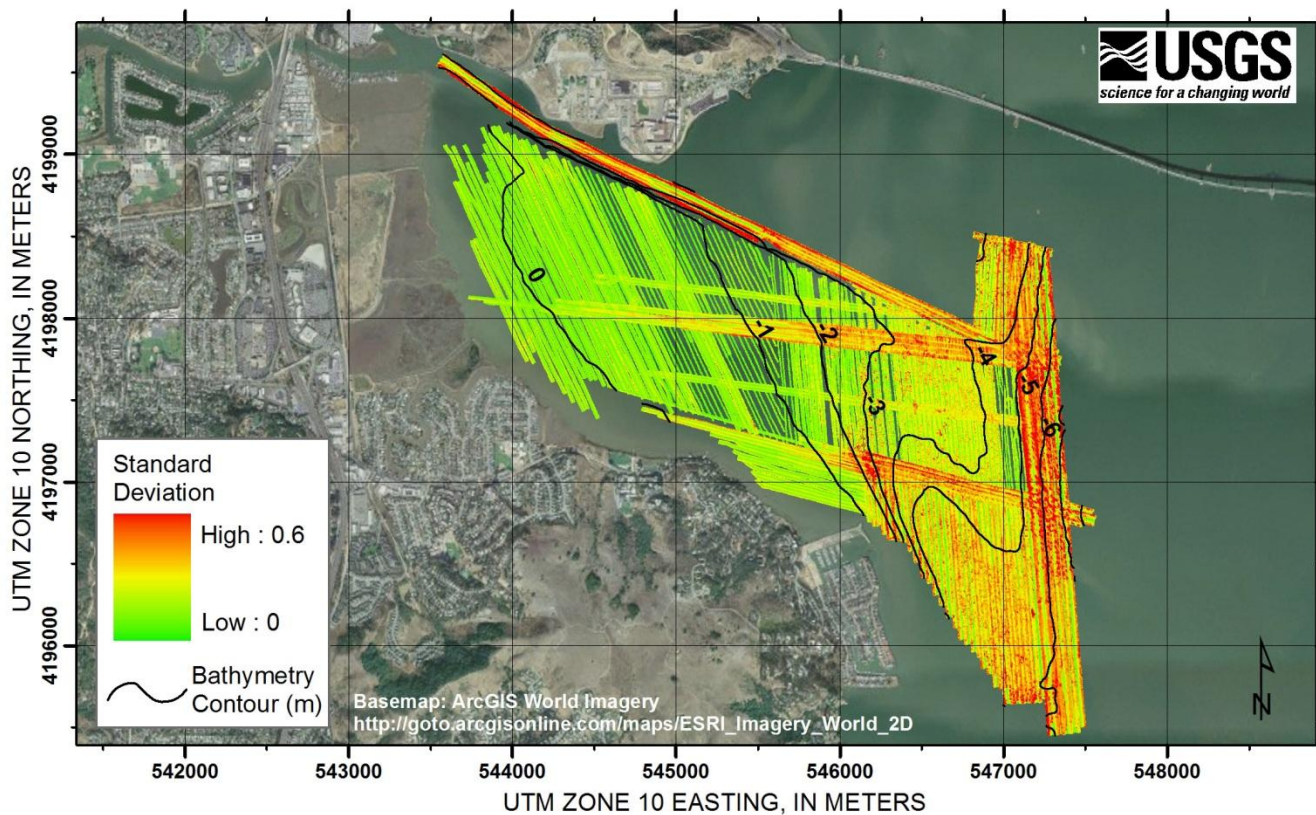


Figure 9. Plan-view map of the bathymetric soundings standard deviation within each 1 by 1 m cell, Corte Madera Bay, California.

The IHO defines several survey orders based on a combination of coverage, depth, and accuracy (IHO, 2008). The IHO defines maximum allowable total vertical uncertainty (TVU) using a depth-dependent formula with two additional variables as defined below (from IHO Standards for Hydrographic Surveys 5th Edition):

$$\pm \sqrt{a^2 + (b \times d)^2} \tag{1}$$

where a represents the portion of the uncertainty that does not vary with depth, b is a coefficient which represents that portion of the uncertainty that varies with depth, and d equals depth.

IHO standards require a 95 percent confidence level, defined as 1.96 times the standard deviation in sounding uncertainty. IHO survey orders use the values found in table 4 as minimums for their survey orders (note that descriptions are generalized, and Order 1 and 1a are combined because they have the same values for minimum TVU). If we assume that the elevation uncertainty in bathymetric soundings is normally distributed, we can estimate the total vertical uncertainty (TVU) in an elevation cell at the 95 percent level using:

$$TVU_{(x,y)} = 1.96 \times \sigma_{(x,y)} \tag{2}$$

where $\sigma_{(x,y)}$ is the standard deviation of all soundings in a cell located at coordinate (x, y) . By comparing the calculated values from equation 2 against the standardized TVU thresholds represented by equation 1, we have an objective measure of the quality of the bathymetric surface.

Table 4. Minimum IHO survey order requirements.

Survey Order	Special	Combined 1 and 1a	2
Description	Areas where under-keel clearance is critical	Areas shallower than 100 meters	Areas generally deeper than 100 meters
Maximum allowable TVU 95% confidence level	a = 0.25 meter b = 0.0075	a = 0.5 meter b = 0.013	a = 1.0 meter b = 0.023

Figure 10 shows a plot of the calculated TVU values (equation 2) for a representative subset of the survey as a function of water depth. For reference, lines indicating the IHO thresholds for Special Order, First Order, and Second Order surveys derived from equation 1 also are displayed. The vast majority of elevation uncertainty in the data set satisfies the IHO standard for First Order surveys, the same standard that the National Oceanic and Atmospheric Administration's (NOAA) National Ocean Service follows, and serves as a testament to the quality of the survey.

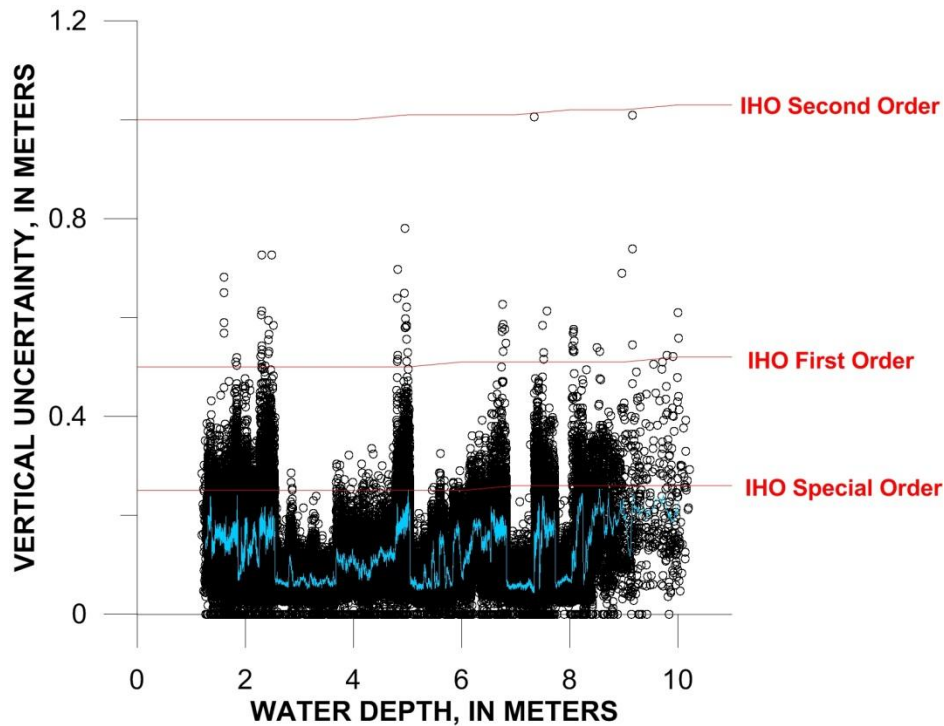


Figure 10. Uncertainty in sounding elevation compared to IHO standards as a function of water depth (approximated to mean high water), Corte Madera Bay, California. For clarity, only 0.1 percent of the data set (randomly selected) is shown out of a total 5.2 million cells in the DEM. The maximum vertical uncertainty allowed for each International Hydrographic Organization survey order is plotted as red lines along with the running average vertical uncertainty of the data set shown in cyan.

Digital Elevation Model Production

Bathymetric Grids

The cleaned and filtered BASE surface was exported from CARIS at 1-m resolution and converted to elevations relative to NAVD88 using the procedures outlined above. Three derivations of the bathymetric grid are provided to fit the varying needs of the end users.

- 1) A 1-m resolution BASE surface created in CARIS using a swath angle weighting scheme where higher weight is given to soundings from the inner part of a swath than to outer beams from adjacent tracklines. This data set is the original bathymetry with datum conversions applied. No additional smoothing or interpolation has been applied so some small-scale ripple features are distinguishable on the bed floor, but gaps exist near nadir and between tracklines.
- 2) A 1-m resolution grid which has been interpolated to fill gaps between tracklines. The 1-m resolution BASE surface was exported from CARIS to an ASCII text file, datum conversions were applied, and the data then imported into Fledermaus for interpolation using a weighted moving average gridding algorithm with a weight diameter of 100 m.
- 3) A 10-m resolution grid. The 1-m resolution BASE surface was exported from CARIS to an ASCII text file, datum conversions were applied, and the data was then imported into Fledermaus for interpolation at 10 m cell size using a weighted moving average gridding algorithm with a weight diameter of 80 m (8 cells).

Lidar Data

The National Oceanic and Atmospheric Administration's Coastal Services Center contracted the acquisition of aerial topographic lidar by Fugro EarthData, Inc., which happened to cover our study area, in the spring of 2010. NOAA's Northern San Francisco Bay aerial lidar was collected from February 25 to April 16, 2010, using a Piper Navajo twin engine aircraft equipped with a Leica ALS60 lidar system. Acquisition was designed to support a nominal point spacing of 1 meter and was collected at low tide to optimize coverage of the intertidal flats. Lidar data was processed by Fugro to achieve a bare-earth ground surface and was provided as 1-m resolution hydro-flattened grids. The stated horizontal accuracy of the lidar is 1 meter RMSE or better. When Fugro compared the lidar to survey grade-GPS points in generally flat, nonvegetated areas the vertical accuracy of 95 percent of the positions had errors less than or equal to 18 cm (equivalent to a 9 cm RMSE, if evenly distributed). The lidar is projected in UTM coordinate space, zone 10. The vertical datum is NAVD88, and the horizontal datum is NAD83 (NSRS2007). Within our study area, NAD83 (NSRS2007) closely approximates the horizontal datum of the bathymetric data, NAD83 (CORS96), and is within the accuracy of the data. For our purposes the two versions of NAD83 are considered equivalent. For additional information on NOAA's Northern San Francisco Bay lidar data set or to download the data directly visit NOAA's CSC Web site: <http://www.csc.noaa.gov/ldart>.

Bathymetric / Topographic DEM

Prior to merging the bathymetry with the topographic lidar a comparison was made between elevations of the two independent data sets where they overlap in the intertidal flats. There is approximately 470,000 m² of overlap between lidar and bathymetry within Corte Madera Bay. The bathymetry is a maximum of 27 cm higher than, or 24 cm lower than, the lidar in the region of overlap. The average difference is 0 cm (SD=4), which suggests that there is not a consistent offset or bias between the two data sets (fig. 11). The 1-m resolution bathymetric grid (interpolated to fill gaps between tracklines) was merged with the topographic lidar using the blend algorithm in the "Mosaic to New Raster" tool in Arc Toolbox (fig. 12). The resultant DEM is provided at 1 m resolution and also was also resampled to 10 m resolution using a bilinear interpolation.

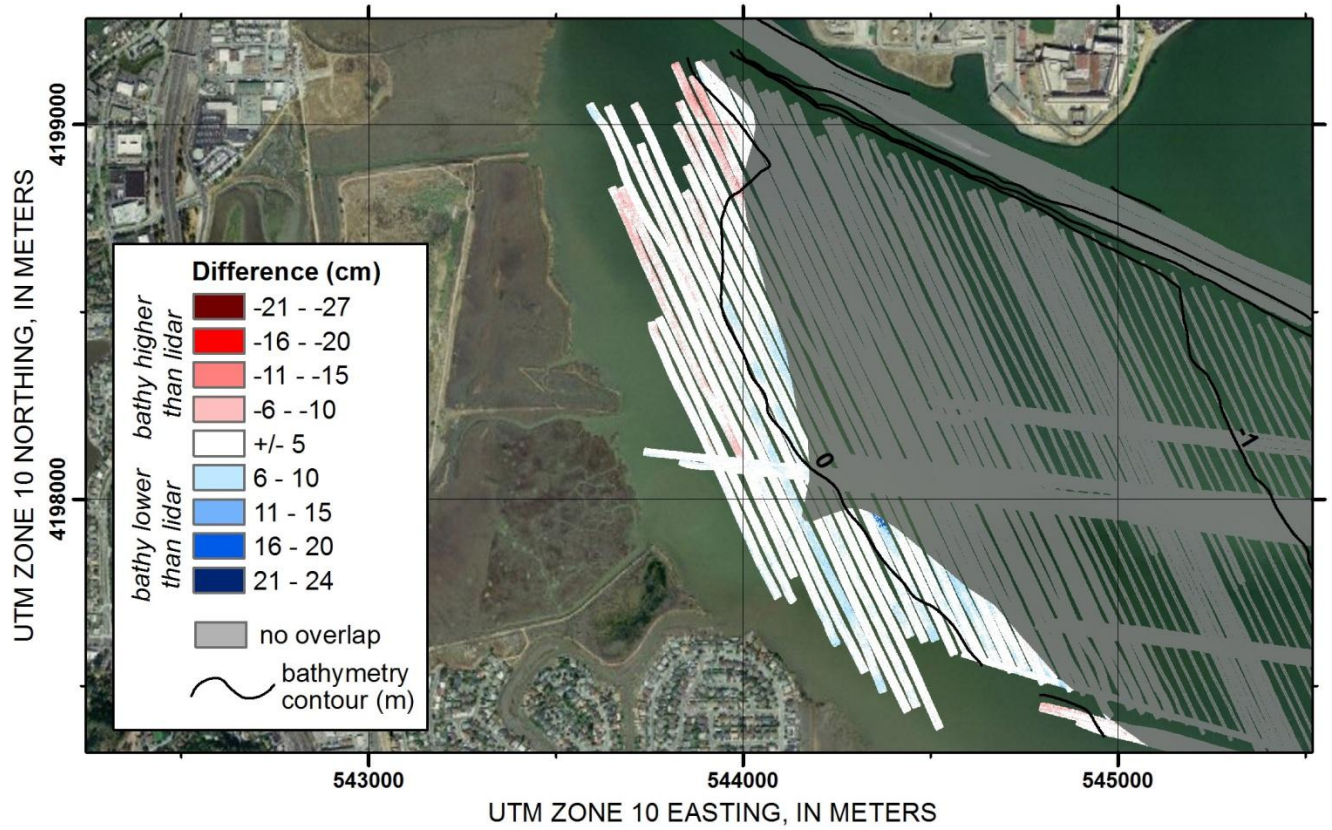


Figure 11. Difference between tidal flat elevations calculated from aerial lidar versus bathymetry, Corte Madera Bay, California.

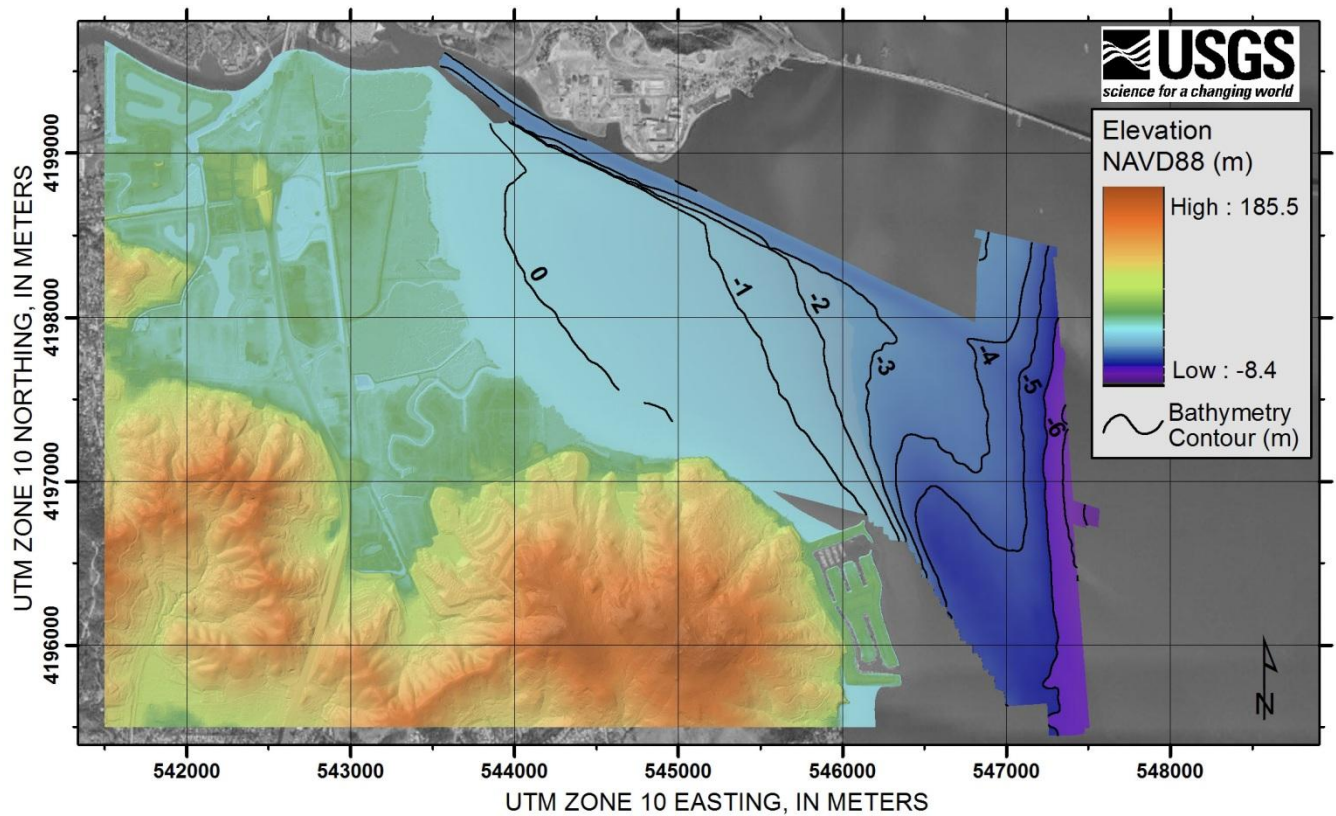


Figure 12. Seamless bathymetric/topographic DEM of Corte Madera, California.

Evaluation of Lidar Bare Earth Elevations in Marsh Vegetation

The ability of aerial lidar to capture bare earth in vegetated areas is largely dependent upon the density of vegetation at a given site. In a separate study, scientists at the USGS Western Ecological Research Center collected measurements of ground elevation throughout the marsh within our study area using a Leica RTK GPS unit with a published vertical and horizontal accuracy of ± 3 cm. More than 700 elevation measurements were collected in March of 2010; points were taken approximately every 25 meters along shore-parallel transects with a nominal spacing of approximately 50 meters between transects. The RTK ground measurements were differenced from the bare earth lidar elevations to evaluate lidar penetration into the vegetation at this site and thus how well the bare earth model performs in the vegetated marsh regions. There was a mean positive offset of 23 cm between the two measurements, indicating that the bare earth lidar in this marsh is, on average, 23 cm (SD=10) higher than the elevations obtained by RTK measurements. Depending upon the particular needs of the end-user, this bias in bare earth elevations in the marsh may or may not be significant. We have divided the marsh into three regions to quantify spatial variations between lidar and RTK measurements in the northern, central, and southern reaches of the marsh (fig. 13). The statistics from this analysis are provided in table 5 so that the end-user may apply adjustments as needed.

Table 5. Difference statistics between real time kinematic (RTK) measurements and bare earth lidar elevations in the marsh. Positive differences indicate that the lidar elevation is higher than the RTK measurement.

	Northern	Central	Southern	Total
Number of Measurements	264	156	324	744
Difference Statistics				
Minimum (cm)	-20	-6	-41	-41
Maximum (cm)	41	45	44	45
Mean (cm)	18	27	26	23
Standard Deviation (cm)	9	7	9	10
Estimated RMSE (cm)	20	28	27	25

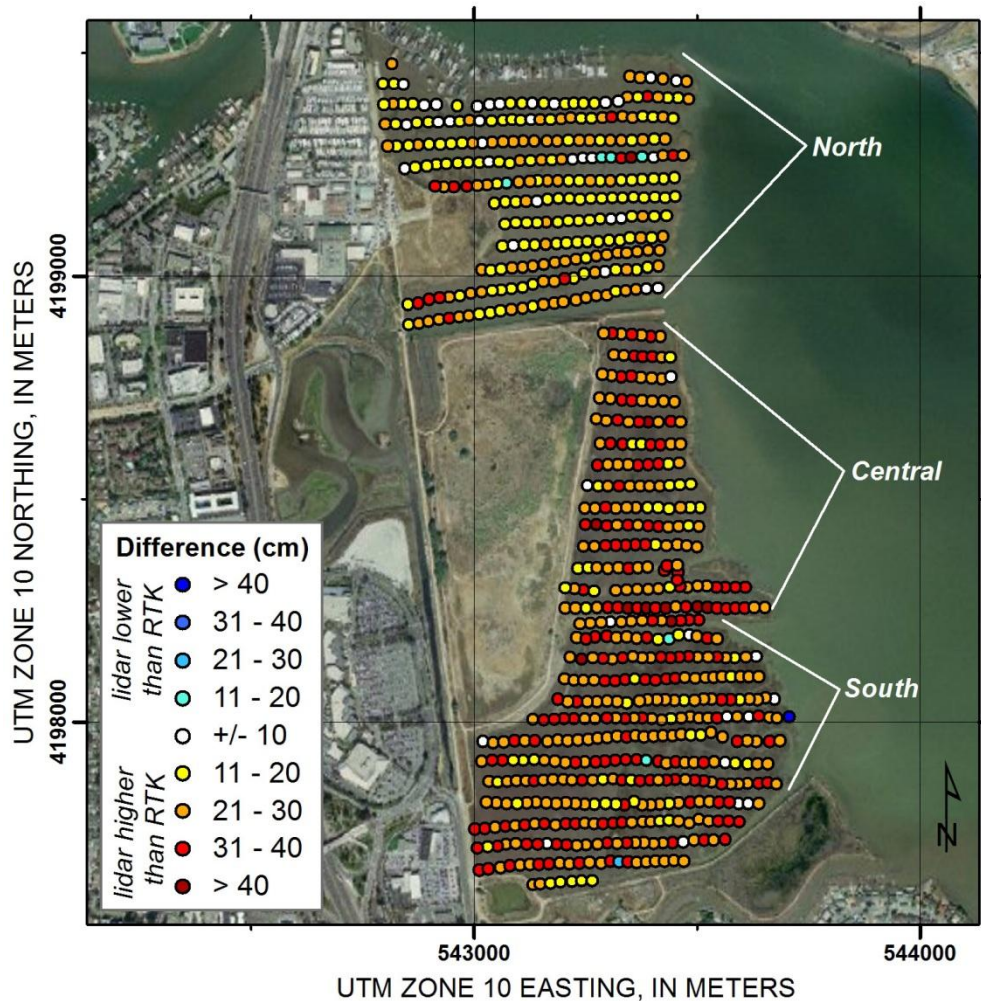


Figure 13. Real time kinematic (RTK) measurements colored by difference between ground elevations as determined by RTK survey versus bare earth lidar DEM, Cortez Madera Bay, California.

Data Tables

A Note on Coordinate Systems and Datums

WGS84 and NAD83 have been revised several times resulting in coordinate shifts of up to several meters in X, Y, and Z. The revision is indicated by the designator following the name (G1150 following WGS84, for example). Software that does not distinguish between the different versions of these datums likely does not support 3D datum properly. Users should pay particular attention to the accompanying metadata files to ensure that the data are properly georeferenced. In particular, note that most current GIS software (including ArcGIS 10) cannot properly transform high-resolution elevation data from one 3D datum to another (such as WGS84 G1150 to NAD83 CORS96) without introducing errors on the order of 1 to 2 m in X, Y, and Z. For this reason, data are provided in both WGS84 G1150 (equivalent to ITRF2000) and NAD83 CORS96 (equivalent to NSRS2007). The geodetic vertical datum of NAVD88 closely approximates the tidal datum of mean lower low water (MLLW) in Corte Madera Bay. VDatum conversions within our study area show that the datum of MLLW is, on average, 3 cm below the datum of NAVD88, however, estimates vary spatially from 12 cm below to 7 cm above the datum of NAVD88.

Bathymetry

Bathymetry data are provided as elevation in meters relative to both the ellipsoid WGS84(G1150) and as orthometric heights NAD83(CORS96)/NAVD88 (table 6). All data are projected in UTM zone 10 North, and all values (eastings, northings, and elevation) are in meters. Each zip file contains the data formatted as both ASCII X, Y, Z text files (*.txt) and ESRI ASCII GRID files (*.asc; see appendix), as well as Federal Geographic Data Committee (FGDC) compliant metadata in both text and .xml format.

Table 6. Bathymetric data files provided.

File name	Horizontal resolution, in meters	Reference frame	Vertical datum
Corte_Madera_bathy_raw_1m_NAVD88.zip	1	NAD83 (CORS96)	NAVD88
Corte_Madera_bathy_raw_1m_WGS84.zip	1	WGS84(G1150)	WGS84(G1150)
Corte_Madera_bathy_interp_1m_NAVD88.zip	1	NAD83 (CORS96)	NAVD88
Corte_Madera_bathy_interp_1m_WGS84.zip	1	WGS84(G1150)	WGS84(G1150)
Corte_Madera_bathy_10m_NAVD88.zip	10	NAD83 (CORS96)	NAVD88
Corte_Madera_bathy_10m_WGS84.zip	10	WGS84(G1150)	WGS84(G1150)

Bathymetric / Topographic DEM

Seamless bathymetric/topographic DEMs are provided as elevations in meters relative to both the ellipsoid WGS84(G1150) and as orthometric heights NAD83(CORS96)/NAVD88 (table 7). All data are projected in UTM, zone 10 North, and all values (eastings, northings, and elevation) are in meters. Each zip file contains the data formatted as both ASCII X, Y, Z text files (*.txt) and ESRI ASCII GRID files (*.asc; see appendix), as well as FGDC-compliant metadata in both text and .xml format. The DEMs are provided as both 1 m and 10 m resolution grids.

Table 7. Bathymetric/topographic DEM files provided.

File name	Horizontal resolution, in meters	Reference frame	Vertical datum
Corte_Madera_topobathy_DEM_NAVD88_1m.zip	1	NAD83 (CORS96)	NAVD88
Corte_Madera_topobathy_DEM_NAVD88_10m.zip	10	NAD83 (CORS96)	NAVD88

Acknowledgments

Thanks to the survey crew of the RV *Snavehy*: Mike Boyle, Greg Gabel, and Pete Dal Ferro (all of the USGS) who assisted with the bathymetry collection and to Tom Reiss who established GPS base stations for the bathymetric surveys. Paul Elsen, Tony Henner, and Kevin Buffington (all of USGS Western Ecological Research Center) assisted with collection and processing of RTK measurements in the marsh. The bathymetry was collected in support of the Innovative Wetland Adaption in the Lower Corte Madera Creek Watershed Project initiated by the San Francisco Bay Conservation and Development Commission and funded by the U.S. Environmental Protection Agency with additional support provided by the USGS Coastal and Marine Geology Program.

References Cited

- Applied Microsystems Ltd., 2005, SVplus sound velocity, temperature, and depth profiler—User’s manual, revision 1.23: 2071 Malaview Ave. Sidney, B.C., Canada, V8L5X6.
- International Hydrographic Organization (IHO), 2008, IHO standards for hydrographic surveys (5th ed.): Special publication 44, International Hydrographic Bureau, Monaco.
- Gann, J.T., 1992, YoNav—your own integrated navigation system for DOS platforms: U.S. Geological Survey, Open File Report 92–565, 48 p., available at <http://pubs.usgs.gov/of/1992/0565/report.pdf>.
- National Geodetic Survey, NOAA, 2009, GEOID09 geoid model, 1315 East-West Highway, Silver Spring, MD 20910–3282, available at <http://www.ngs.noaa.gov/GEOID/GEOID09/>.
- Systems Engineering & Assessment (SEA) Ltd., 2004, SWATHplus training pack: Beckington Castle, P.O. Box 800, Frome, England, BA11 6TB.
- Soler, T., and Snay, R.A., 2004, Transforming positions and velocities between the International Terrestrial Reference Frame of 2000 and North American Datum of 1983: *Journal of Surveying Engineering*, May 2004 (49).

Appendix

Description of the ESRI ASCII Grid raster format:

To import ASCII Grids into common GIS packages:

ArcGIS: Use ArcTools's Import ASCII to GRID function

ArcView: Use the import ASCII Grid function (May need Spatial Analyst)

GRASS: Use the 'r.in.arc' function.

The ASCII file consists of header information containing a set of keywords, followed by cell values in row-major order. The file format is:

```
<NCOLS xxx>
<NROWS xxx>
<XLLCENTER xxx | XLLCORNER xxx>
<YLLCENTER xxx | YLLCORNER xxx>
<CELLSIZE xxx>
{NODATA_VALUE xxx}
row 1
row 2
.
.
.
row n
```

where xxx is a number, and the keyword nodata_value is optional and defaults to -9999. Row 1 of the data is at the top of the grid, row 2 is just under row 1 and so on. The nodata_value is the value in the ASCII file to be assigned to those cells whose true value is unknown. In the grid they will be assigned the keyword NODATA. Cell values are delimited by spaces. No carriage returns are necessary at the end of each row in the grid (although they are included in this case). The number of columns in the header is used to determine when a new row begins. The number of cell values is equal to the number of rows times the number of columns.